Published in final edited form as:
Nat Cell Biol. ; 13(10): 1252–1258. doi:10.1038/ncb2320.

Dynamic maintenance of asymmetric meiotic spindle position through Arp2/3 complex-driven cytoplasmic streaming in mouse oocytes

Kexi Yi[a], **Jay R. Unruh**[a], **Manqi Deng**[b], **Brian D. Slaughter**[a], **Boris Rubinstein**[a], and **Rong Li**[a,c]

[a]Stowers Institute for Medical Research, 1000 East 50th Street, Kansas City, MO 64110

[b]Department of Obstetrics and Gynecology and Reproductive Biology, Brigham and Women's Hospital, Harvard Medical School, Boston, MA 02115

[c]Department of Molecular and Integrative Physiology, University of Kansas Medical Center, 3901 Rainbow Boulevard, Kansas City, KS 66160

Abstract

Mature mammalian oocytes are poised for the completion of second polar body extrusion upon fertilization by positioning the metaphase spindle in close proximity to an actomyosin-rich cortical cap. Loss of this spindle position asymmetry is often associated with poor oocyte quality and infertility [1–3]. Here, we report a novel role for the Arp2/3 actin nucleation complex in the maintenance of asymmetric spindle position in mature mouse oocytes. The Arp2/3 complex localizes to the cortical cap in a Ran GTPase-dependent manner and accounts for the nucleation of the majority of actin filaments in both the cortical cap and a cytoplasmic actin network. Inhibition of Arp2/3 complex activity or localization leads to rapid dissociation of the spindle from the cortex. High resolution live imaging and spatiotemporal image correlation spectroscopy (STICS) analysis reveal that in normal oocytes actin filaments flow continuously away from the Arp2/3-rich cortex, generating a cytoplamic streaming that results in a net pushing force on the spindle toward the actomyosin cap. Arp2/3 inhibition not only diminishes this actin flow and cytoplamic streaming but also enables a reverse streaming driven by myosin-II-based cortical contraction, leading to spindle movement away from the cortex. We conclude that the Arp2/3 complex maintains asymmetric meiotic spindle position by generating an actin polymerization-driven cytoplamic streaming and by suppressing a counteracting force from myosin-II-based contractility.

Maturation of mammalian oocytes involves two consecutive and highly asymmetric meiotic divisions, giving rise to a large haploid egg and two much smaller polar bodies [4]. These asymmetric divisions require the meiotic spindle to be positioned closely to the cortical region where polar body extrusion occurs. Previous studies have shown that the initial establishment of asymmetric spindle positioning in meiosis I (MI) relies on an actin-dependent migration process, through which the spindle relocates from the center of the oocyte to a position near the cortex [5–7]. The cortical proximity enables the meiotic chromatin to signal the assembly of a membrane domain, consisting of an actin cap

AUTHOR CONTRIBUTIONS

K.Y. and R.L. designed the experiments, interpreted results and wrote the paper; K.Y. carried out all the experiments except DNA-beads experiment, which was performed by M.D.; J.U. contributed to data analysis including STICS with assistance from B.S.; B.R. performed the numerical simulations; R.L. coordinated and supervised the whole project.

COMPETING INTERESTS

The authors declare no competing financial interests.

surrounded by a ring of myosin-II, instrumental for polar body extrusion and abscission [8,9]. In Meiosis II (MII), the 2nd meiotic spindle assembles around the chromosomes already positioned near the cortex after the 1st polar body extrusion. The asymmetrically positioned MII spindle/chromosomes induce and maintain the actomyosin cap required for the 2nd polar body extrusion [8]. In most vertebrate species including mammals, the mature oocyte may arrest in MII for hours to days awaiting fertilization [10], during which the asymmetric positioning of the MII spindle/chromosomes must be stably maintained to ensure immediate extrusion of the 2nd polar body upon sperm penetration.

Although asymmetric positioning of the MII spindle is a well recognized indicator for high oocyte quality, and oocytes from aged females with declined fertility often exhibit a spindle far away from the cortex [2,3], little is known about the molecular mechanism for maintaining spindle position during the prolonged meiotic arrest. Whereas in many types of asymmetrically dividing mitotic cells the spindle position/orientation is known to be accomplished by microtubules and their associated motor proteins [11], disrupting microtubules does not affect the subcortical location of MII chromatin [8]. Early studies in mouse oocytes showed that cytochalasin B, an actin inhibitor, blocks the spindle rotation that occurs during the 2nd polar body extrusion [12], hinting at the possibility that actin as opposed to microtubules may serve as a connection between the MII spindle and the cortex. More recently it was shown that the MII spindle is detached from the cortex when Rac activity is perturbed [13], further pointing to a possible role for actin in maintaining MII spindle position asymmetry.

To directly test whether actin is required for the maintenance of asymmetric MII spindle position, we incubated mouse oocytes with the available chemical inhibitors of the actin cytoskeleton, including latrunculin A (LatA), an inhibitor of actin polymerization [14], blebbistatin, inhibiting myosin-II ATPase activity [15], and CK-666 [16], the recently discovered inhibitor of the Arp2/3 complex, an actin nucleating factor widely involved in cell motility and membrane trafficking [17]. Interestingly, among these three inhibitors, only CK-666 potently disrupted the sub-cortical spindle position. In 60.25 ± 3.32% MII oocytes (n=68) treated with 50 μM CK-666, the spindles were found to be detached from the cortex and were instead positioned near the center of the oocytes (Fig. 1a and c), while 95.35% of control oocytes (n=51) maintained a subcortically located spindle. The effect of CK-666 was specific to the maintenance of the asymmetric spindle position in MII oocytes, because MI spindle migrated successfully to the cortex in the majority of MII oocytes (82.61%, n= 23) treated with CK-666 (Fig. S1). However, because MI completes soon after this migration, it is unclear if CK-666 would affect a prolonged maintenance of MI spindle at the cortex.

To confirm the MII spindle positioning defect caused by CK-666 treatment was indeed due to inhibition of Arp2/3 complex activity, we injected MII oocytes with mRNA encoding two tandem CA domains (2CA) from N-WASP, an activator of the Arp2/3 complex [18]. The CA domain binds to but does not activate the Arp2/3 complex, thus exerting a dominant negative effect. The tandem construct was designed to enhance the dominant negative effect by increasing the affinity with the Arp2/3 complex. As a negative control, 2(CA^{W55A}), a construct of tandem copies of CA bearing the W55A mutation, known to demolish the affinity with the Arp2/3 complex [19], was used. As shown in Fig. 1c, expression of 2CA in mouse oocytes by RNA injection induced significant spindle positioning defect compared to 2(CA^{W55A}) expressing and H_2O (solvent for the RNA)-injected control oocytes (n=38). Taken together, the above data suggest that the actin nucleation activity of the Arp2/3 complex is required for the maintenance of asymmetric positioning of MII spindle (the seemingly contradictive observation that LatA does not disrupt asymmetric spindle location is explained below). By contrast, formin-2 (Fmn2), a formin family actin nucleating protein, was previously shown to be required for the initial spindle migration to the cortex in MI

oocytes [20–22], but Fmn2 is not required for the maintenance of a cortical spindle location, as injection of DNA-coated beads to a subcortical location in Fmn2−/− oocytes maintains such location and stimulated the formation of a spindle and an actomyosin cap in the overlying cortex (Fig.S2).

Spindle relocation to the center of the oocytes could be observed within an hour after CK-666 addition. Considering the large size of the spindle and the viscosity of the cytoplasm, spindle movement away from the cortex is likely to be driven by an active force. To observe this process more closely, we imaged the MII chromosome movement by video microscopy after CK-666 addition. Indeed, within 5 min after the drug addition, the spindle exhibited directed movement away from the cortical cap region, toward the oocyte center at an average speed of 0.32±0.07 μm/min (n=6) (Fig. 1b and Movie S1). Because the cortical cap is rich in actin and myosin-II and the spindle movement induced by CK-666 was often accompanied by an apparent contraction of the cortical cap region (see below), we tested the effect of blebbistatin on this spindle movement. Whereas blebbistatin alone had no effect on spindle position, it prevented spindle detachment from the cortex in the presence of CK-666 (Fig.1a, b and Movie S2), suggesting that myosin-II contractility was responsible for the spindle movement away from the cortex when the Arp2/3 complex is inhibited. This result also explains the apparent paradox that LatA treatment does not readily alter spindle position, as LatA disrupts both Arp2/3- mediated actin assembly and contractile actomyosin structures. Interestingly, while disruption of microtubules with nocodazol had no effect on meiotic chromosome position on its own, this treatment prevented the chromosome from detaching from the cortical cap upon CK-666 incubation and the chromosomes appeared tightly associated with the cortex (Fig.1a).

To investigate how the Arp2/3 complex maintains spindle position, we next examined the localization of Arp2/3 complex in MII mouse oocytes. Immuno-staining with a polyclonal anti-Arp2 antibody showed localization of Arp2 to the cortical actin cap overlying the spindle (Fig. 2a). Cortical cap localization of the Arp2/3 complex was further confirmed by expression of EGFP-Arp3 via RNA injection (Fig. 2a). Our previous work showed that meiotic chromatin, when positioned in proximity to the cortex of an MII oocyte, induces the formation of a cortical actin cap through Ran GTPase signaling [8]. We therefore examined if the Ran signal also regulates Arp2/3 complex localization at the cortical cap. MII oocytes were injected with a dominant negative Ran protein, Ran^{T24N}, which inhibits activation of the endogenous Ran by the guanine nucleotide exchange factor RCC1 [23]. Ran^{T24N} disrupted asymmetric positioning of MII spindle in 70.97% (n=31) of the injected MII oocytes, recapitulating the effect of Arp2/3 inactivation, whereas injection of wild-type Ran protein or buffer alone had no effect (Fig.2b). Although the cortical localization of Arp2 was also disrupted in the Ran^{T24N}–injected oocytes where the spindle had moved away from the cortex, this could simply be a consequence of the increased distance between chromosomes and the cortex rather than a direct effect of Ran inhibition. To clarify this, nocodazole was added to the culture medium for Ran^{T24N} injected oocytes. Nocodazol addition prevented chromosome detachment from the cortex; however, Arp2 was still delocalized from the cortical cap (Fig. 2c). In contrast, Arp2 showed normal localization at the cortical cap in Ran WT injected oocytes, as well as in buffer injected control oocytes. Thus, the Ran GTPase, activated by the chromatin-associated RCC1, regulates Arp2/3 complex localization to the chromatin-proximal cortex, while the Arp2/3 complex in turn plays a key role in maintaining the sub-cortical positioning of chromosomes/spindle.

To further understand how the Arp2/3 complex-regulated actin assembly controls spindle position, we examined the effect of Arp2/3 inhibition on actin organization in mouse oocytes. First, the cortical cap localization of Arp2/3 complex indicates that it may nucleate actin assembly in this region. Most of the oocytes treated with CK-666 no longer retained

the cortical actin cap, as expected considering the diminished chromatin signal after the spindle movement away from the cortex. However, even in those remaining oocytes with spindles still located subcortically after CK-666 treatment, the actin cap was significantly diminished as revealed by phalloidin staining (Fig. 3a and b), while myosin-II remained associated with the same cortical region as a cap instead of a ring normally observed around the actin cap (Fig. 3a). Inhibition of actin assembly in the cortical cap by CK-666 was further confirmed in nocodazole-treated oocytes where the chromatin stayed in close contact with the cortex (Fig. 3b). Loss of the cortical actin cap was also observed in nocodazol treated oocytes expressing the inhibitory 2CA peptide but not the control 2(CA^{W55A}) peptide (Fig. 3c), or expressing Ran^{T24N} (Fig. 2d). These results demonstrate that the Arp2/3 complex is responsible for the generation of a majority of the F-actin in the cortical cap and is required for the maintenance of a myosin-II-clear zone in the center of the cap. Interestingly, despite a drastic reduction in cortical actin cap intensity, we noticed a weak F-actin enrichment at the cap persistent even at high CK-666 concentrations (Fig. 3a, arrow), indicating the possible presence of other actin nucleation factors.

Recent work in MI mouse oocytes using live F-actin probes revealed the presence of dynamic cytoplasmic actin structures, which play crucial roles in spindle migration but were difficult to observe in fixed oocytes by phalloidin staining [20–22]. One such probe, UtrCH-GFP, was instrumental for the observation of an extensive cytoplamic actin network connected with the MI spindle [24]. We expressed UtrCH-GFP in MII mouse oocytes and observed a similarly extensive F-actin network that can be disrupted by LatA (Fig.S3). Interestingly, unlike in MI oocytes where the cytoplamic F-actin network is dependent on Fmn2, the MII cytoplasmic actin network was grossly disrupted by CK-666 treatment (Fig.S3), suggesting that the Arp2/3 complex may also be responsible for the assembly of this actin network. We next observed the dynamics of the cytoplamic actin network in oocytes expressing UtrCH-GFP by performing high-resolution time-lapse confocal microscopy. Tracking of the movement of distinct actin structures near the cortical cap first showed a continuous flow of actin structures away from the cortical cap (Fig. 4a and Movie S3).

To quantitatively observe actin flow over the entire oocyte, we performed spatiotemporal image correlation spectroscopy (STICS) analysis [25], which allows measurements of velocity vectors from spatial and temporal correlations of fluorescence intensity fluctuations from confocal image series. STICS analysis showed that the actin flow initiates with the highest magnitude (0.4 μm/sec) from the cortical cap, down along both sides of the lateral cortex, and converge at the center of the oocytes in the reverse direction toward the spindle (Fig. 4b). CK-666 treatment attenuates the high rate of actin flow from the cortical cap (Fig. 5a and see below for further explanation). The observed actin flow is reminiscent of the actin retrograde flow at the leading edge of keratocytes or fibroblasts, which results from spatially separate actin nucleation and turnover [26]. Indeed, cofilin, the highly conserved actin depolymerizing factor [27], was found to “coat” the spindle, as detected by immunofluoresence staining using two independent antibodies (Fig. S4). Furthermore, staining with an antibody specific for the phosphorylated (thus inactive) cofilin did not show the same localization, suggesting that the spindle surface is enriched for active cofilin (Fig. S4).

During the above imaging of actin dynamics, we noticed coordinated movement of cytoplasmic particles of various size and appearance under the differential interference contrast (DIC) channel. These particles exhibited streaming in a swirling pattern that can be easily seen in a time-projected image (Fig. 4b and also seen in Movie S3). Cytoplasmic particles streamed away from the cortical cap region along the cell periphery, arrived at the opposite pole of the oocyte, and then circulated back in the central part of the oocyte toward

the spindle (Fig.4b). STICS analysis showed that the pattern of cytoplasmic particle movement correlated well with the actin flow (Fig.4b). LatA treatment of the oocytes completely disrupted the observed cytoplasmic streaming, suggesting that it is dependent on F-actin assembly (Fig. S5).

Fluid dynamics simulation suggests that the above described cytoplasmic streaming is able to generate a net pressure on the spindle toward the cortex (Fig. 4c,d). Consistent with this possibility, immediately after spindle disassembly due to nocodazole treatment, the naked chromosomes can be seen to be pushed toward the cortex at the same speed as cytoplasmic particles in the vicinity, until the chromatin was tightly against the cortex (Fig. 4e). To further test the possibility that cytoplasmic streaming pushes the spindle toward the cortex, we briefly treated oocytes with CK-666 (~20 min) such that the spindle began to move away from the cortex. We then transferred the oocytes to drug free media. In oocytes where the spindle had not moved too far away from the cortex, the actin flow-powered cytoplasmic streaming resumed. Concomitantly, the spindle began to move back toward the cortex along with the particles at a similar migration rate (Fig.4f). As the particles observed moved behind the spindle, it was unlikely that their movement was a consequence of spindle movement. This result supports the notion that the actin flow-driven cytoplasmic streaming exerts a force on the spindle, pushing it toward the cortex.

Unexpectedly, CK-666 treatment not only disrupted the observed cytoplasmic streaming but activated a cytoplasmic streaming in the reverse direction: particles now flowed toward the cortical cap along the sides of the oocyte and away from the spindle and in the center of the oocyte (Fig.5a and Movie S4). Importantly, activation of this reverse cytoplasmic streaming after CK-666 addition is tightly coupled with the spindle movement away from the cortex (Fig.5b). Blebbistatin, which prevents spindle detachment induced by CK-666, completely attenuated the reverse cytoplasmic streaming, suggesting that myosin-II contractility drives both spindle detachment and reverse cytoplasmic streaming when Arp2/3 is inhibited (Fig. 5a and Movie S5). Because in Arp2/3-inhibited oocytes myosin-II remains concentrated to the cortical cap with a small amount of residual F-actin (Fig.3a), it is likely that the reverse cytoplasmic streaming is driven by contraction of the cortical cap. This is evident in oocytes expressing UtCH-GFP treated with CK-666: the GFP cap rapidly reduced in size while the intensity near the cap center remained constant (Fig.5c and Movie S6). Another way to visualize cap contraction was to stain the oocyte surface with fluorescently labeled ConA. The cap region exhibited low ConA staining, while the rest of the surface stained strongly with ConA. Contraction of the ConA-dim zone can be readily observed after CK-666 addition and was blocked by blebbistatin (Fig.5d and Movie S7, S8). Fluid dynamics simulation suggests that the reverse cytoplasmic streaming driven by contraction near the cap region results in a net pressure pushing the spindle away from the cortex (Fig.5e and f).

In conclusion, the experiments presented above demonstrate that the maintenance of asymmetric positioning of the MII spindle in mammalian oocytes is an active process accomplished through dynamic actin assembly. At the completion of meiosis I, the cortically located MII chromosomes, through Ran signaling, localize and activate the Arp2/3 complex at the proximal cortex, establishing the cortical cap. In turn the Arp2/3 complex maintains the chromosomes/spindle close to the cortex, forming a feedback loop maintaining MII oocyte polarity. The Arp2/3 complex's role in maintaining spindle position is two fold. First, the Arp2/3 complex generates a continuous actin flow possibly through actin treadmilling as a result of spatially disparate actin barbed end nucleation/elongation and depolymerization by cofilin concentrated at the spindle surface, much like the proposed array treadmilling at the leading edge of migratory cells [28]. This Arp2/3 generated actin flow drives cytoplasmic streaming in a pattern predicted to result in a net pressure on the spindle surface toward the cortical cap. Second, the Arp2/3 complex nucleated actin assembly prevents myosin-II

driven contraction of the cortical cap. Spindle detachment from the cortex and movement toward the oocyte center can be attributed to cortical cap contraction and a consequent reverse cytoplasmic streaming in the absence of Arp2/3 activity. Interestingly, this myosin-II driven reverse cytoplasmic streaming in oocyte may be reminiscent of the myosin-II-driven fluid flow in fast moving keratocytes [29].

Loss of asymmetric position of spindle/MII chromosomes disrupts oocyte polarity and prevents 2nd polar body extrusion, and is a known cause of impaired reproductive potential in ageing females [2,3,30]. As such, the spindle position is used as a clinical index to evaluate the quality of MII oocytes for in-vitro fertilization [31,32]. Given the importance of maintaining spindle position asymmetry, it is interesting to ponder what evolutionary design principle may underlie a highly active force-generating mechanism, i.e., actin-driven cytoplasmic streaming. After all, it may appear that the sole purpose of the Arp2/3-mediated actin flow is to guard against a spindle-detachment force resulting from cortical cap contraction, as the spindle was observed to stay in place when both actin flow and contractile activity were disrupted by LatA treatment. The answer may lie in the fact that the presence of a contraction-ready myosin-II structure is an important requirement for poising the oocytes to complete the 2nd meiosis immediately upon sperm entry. In addition, maintaining spindle position under an active force provided by the actin flow should prevent slow and random drift of spindle position or orientation during a prolonged meiotic arrest. Finally, we speculate that an active mechanism of spindle position maintenance that requires high energy expenditure (i.e. to support constant actin polymerization and turnover), as opposed to one involving a static tether, may impose a natural and stringent selection for oocytes that possess superior vitality and energy generating potential to undergo zygotic development.

METHODS

Methods and all associated references are available in the online version of the paper at http://www.nature.com/naturecellbiology/

Supplementary Material

Refer to Web version on PubMed Central for supplementary material.

Acknowledgments

We thank W.M. Bement (University of Wisconsin) for providing pCS2+-UtrCH-GFP plasmid; J. Bamburg (Colorado State University) for providing anti-cofilin and phos-cofilin antibodies; H. Cartwright (Stowers Institute, the same with all names mentioned hereafter) for microfabricated wells for oocyte imaging; M. Durnin and K. Westfahl for technical assistance and mice maintenance. This work was supported in part with NIH grant P01 GM 066311.

References

1. Sathananthan AH. Ultrastructure of the human egg. Hum Cell. 1997; 10:21–38. [PubMed: 9234062]
2. Webb M, Howlett SK, Maro B. Parthenogenesis and cytoskeletal organization in ageing mouse eggs. J Embryol Exp Morphol. 1986; 95:131–145. [PubMed: 3794588]
3. Kim NH, Moon SJ, Prather RS, Day BN. Cytoskeletal alteration in aged porcine oocytes and parthenogenesis. Mol Reprod Dev. 1996; 43:513–518. [PubMed: 9052943]
4. Maro B, Johnson MH, Webb M, Flach G. Mechanism of polar body formation in the mouse oocyte: an interaction between the chromosomes, the cytoskeleton and the plasma membrane. J Embryol Exp Morphol. 1986; 92:11–32. [PubMed: 3723057]

5. Longo FJ, Chen DY. Development of cortical polarity in mouse eggs: involvement of the meiotic apparatus. Dev Biol. 1985; 107:382–394. [PubMed: 4038667]
6. Verlhac MH, Lefebvre C, Guillaud P, Rassinier P, Maro B. Asymmetric division in mouse oocytes: with or without Mos. Curr Biol. 2000; 10:1303–1306. [PubMed: 11069114]
7. Leader B, et al. Formin-2, polyploidy, hypofertility and positioning of the meiotic spindle in mouse oocytes. Nat Cell Biol. 2002; 4:921–928. [PubMed: 12447394]
8. Deng M, Suraneni P, Schultz RM, Li R. The Ran GTPase mediates chromatin signaling to control cortical polarity during polar body extrusion in mouse oocytes. Dev Cell. 2007; 12:301–308. [PubMed: 17276346]
9. Deng M, Li R. Sperm chromatin-induced ectopic polar body extrusion in mouse eggs after ICSI and delayed egg activation. PLoS One. 2009; 4:e7171. [PubMed: 19787051]
10. Brunet S, Maro B. Cytoskeleton and cell cycle control during meiotic maturation of the mouse oocyte: integrating time and space. Reproduction. 2005; 130:801–811. [PubMed: 16322540]
11. Siller KH, Doe CQ. Spindle orientation during asymmetric cell division. Nat Cell Biol. 2009; 11:365–374. [PubMed: 19337318]
12. Zhu ZY, et al. Rotation of meiotic spindle is controlled by microfilaments in mouse oocytes. Biol Reprod. 2003; 68:943–946. [PubMed: 12604646]
13. Halet G, Carroll J. Rac activity is polarized and regulates meiotic spindle stability and anchoring in mammalian oocytes. Dev Cell. 2007; 12:309–317. [PubMed: 17276347]
14. Ayscough KR, et al. High rates of actin filament turnover in budding yeast and roles for actin in establishment and maintenance of cell polarity revealed using the actin inhibitor latrunculin-A. J Cell Biol. 1997; 137:399–416. [PubMed: 9128251]
15. Straight AF, et al. Dissecting temporal and spatial control of cytokinesis with a myosin II Inhibitor. Science. 2003; 299:1743–1747. [PubMed: 12637748]
16. Nolen BJ, et al. Characterization of two classes of small molecule inhibitors of Arp2/3 complex. Nature. 2009; 460:1031–1034. [PubMed: 19648907]
17. Goley ED, Welch MD. The ARP2/3 complex: an actin nucleator comes of age. Nat Rev Mol Cell Biol. 2006; 7:713–726. [PubMed: 16990851]
18. Campellone KG, Welch MD. A nucleator arms race: cellular control of actin assembly. Nat Rev Mol Cell Biol. 2010; 11:237–251. [PubMed: 20237478]
19. Higgs HN, Blanchoin L, Pollard TD. Influence of the C terminus of Wiskott-Aldrich syndrome protein (WASp) and the Arp2/3 complex on actin polymerization. Biochemistry. 1999; 38:15212–15222. [PubMed: 10563804]
20. Azoury J, et al. Spindle positioning in mouse oocytes relies on a dynamic meshwork of actin filaments. Curr Biol. 2008; 18:1514–1519. [PubMed: 18848445]
21. Li H, Guo F, Rubinstein B, Li R. Actin-driven chromosomal motility leads to symmetry breaking in mammalian meiotic oocytes. Nat Cell Biol. 2008; 10:1301–1308. [PubMed: 18836438]
22. Schuh M, Ellenberg J. A new model for asymmetric spindle positioning in mouse oocytes. Curr Biol. 2008; 18:1986–1992. [PubMed: 19062278]
23. Wilde A, et al. Ran stimulates spindle assembly by altering microtubule dynamics and the balance of motor activities. Nat Cell Biol. 2001; 3:221–227. [PubMed: 11231570]
24. Burkel BM, von Dassow G, Bement WM. Versatile fluorescent probes for actin filaments based on the actin-binding domain of utrophin. Cell Motil Cytoskeleton. 2007; 64:822–832. [PubMed: 17685442]
25. Hebert B, Costantino S, Wiseman PW. Spatiotemporal image correlation spectroscopy (STICS) theory, verification, and application to protein velocity mapping in living CHO cells. Biophys J. 2005; 88:3601–3614. [PubMed: 15722439]
26. Cramer LP. Molecular mechanism of actin-dependent retrograde flow in lamellipodia of motile cells. Front Biosci. 1997; 2:d260–d270. [PubMed: 9206973]
27. Chen H, Bernstein BW, Bamburg JR. Regulating actin-filament dynamics in vivo. Trends Biochem Sci. 2000; 25:19–23. [PubMed: 10637608]
28. Pollard TD, Borisy GG. Cellular motility driven by assembly and disassembly of actin filaments. Cell. 2003; 112:453–465. [PubMed: 12600310]

29. Keren K, Yam PT, Kinkhabwala A, Mogilner A, Theriot JA. Intracellular fluid flow in rapidly moving cells. Nat Cell Biol. 2009; 11:1219–1224. [PubMed: 19767741]
30. Miao YL, Kikuchi K, Sun QY, Schatten H. Oocyte aging: cellular and molecular changes, developmental potential and reversal possibility. Hum Reprod Update. 2009; 15:573–585. [PubMed: 19429634]
31. Cohen Y, et al. Spindle imaging: a new marker for optimal timing of ICSI? Hum Reprod. 2004; 19:649–654. [PubMed: 14998965]
32. Moon JH, et al. Visualization of the metaphase II meiotic spindle in living human oocytes using the Polscope enables the prediction of embryonic developmental competence after ICSI. Hum Reprod. 2003; 18:817–820. [PubMed: 12660277]

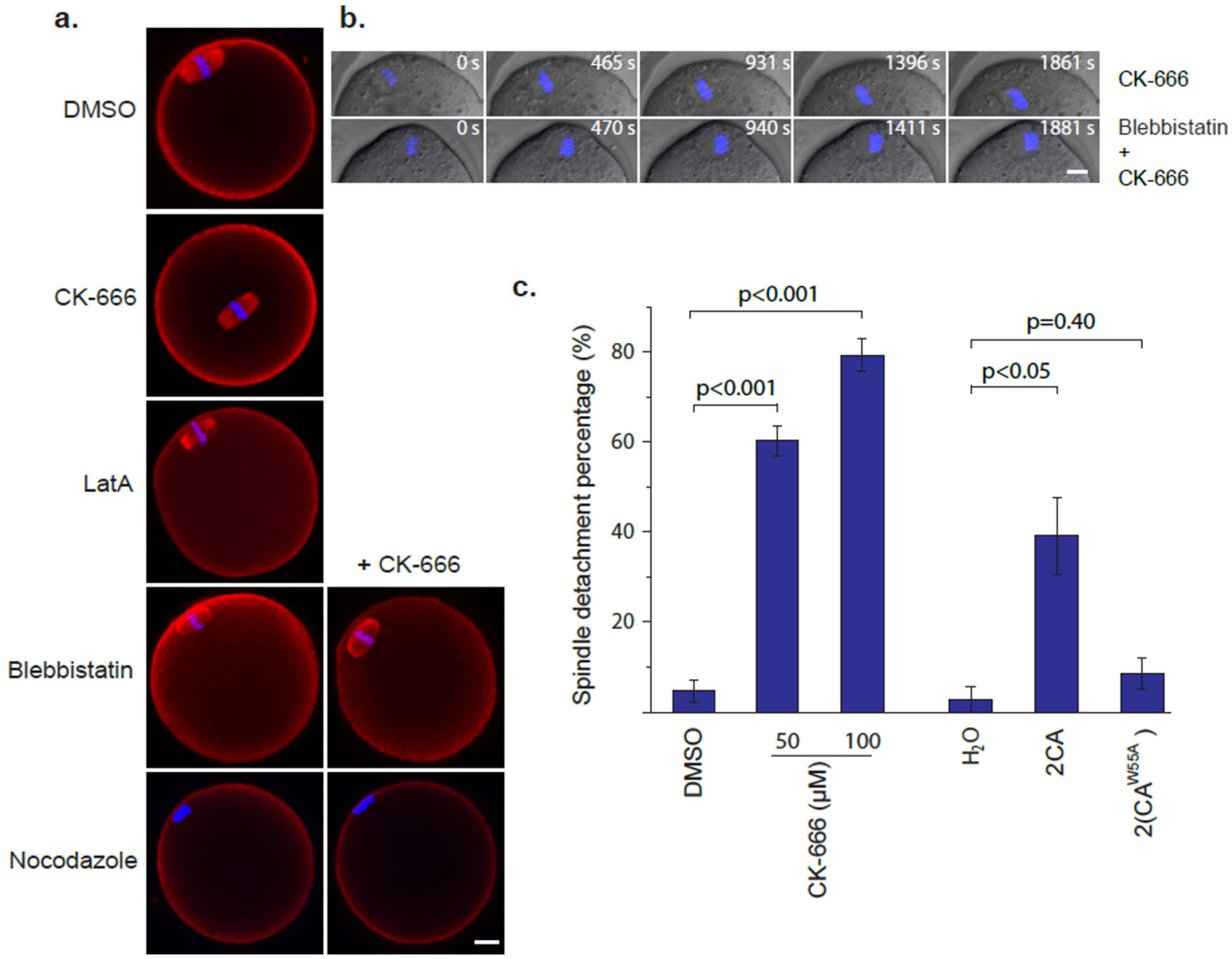

Figure 1. Inhibition of Arp2/3 complex activity disrupts asymmetric MII spindle position

(a) Representative images of MII spindle position after different drug treatments. The Arp2/3 inhibitor CK-666 induced spindle detachment from the cortex towards the cell center. The bottom four panels show effects of blebbistatin and nocodazole on CK-666-induced spindle centralization. Scale bar: 10 μm. (b) Time-lapse imaging of chromosome movement in MII oocytes treated with 50 μM CK-666, or 50 μM CK-666 with 100 μM Blebbistatin. Scale bar: 10 μm. (c) Quantification of spindle detachment percentage after inhibiting Arp2/3 activity by either CK-666 or 2CA mRNA injection. Data are mean±s.e.m (3 experiments, 22–52 oocytes/experiment).

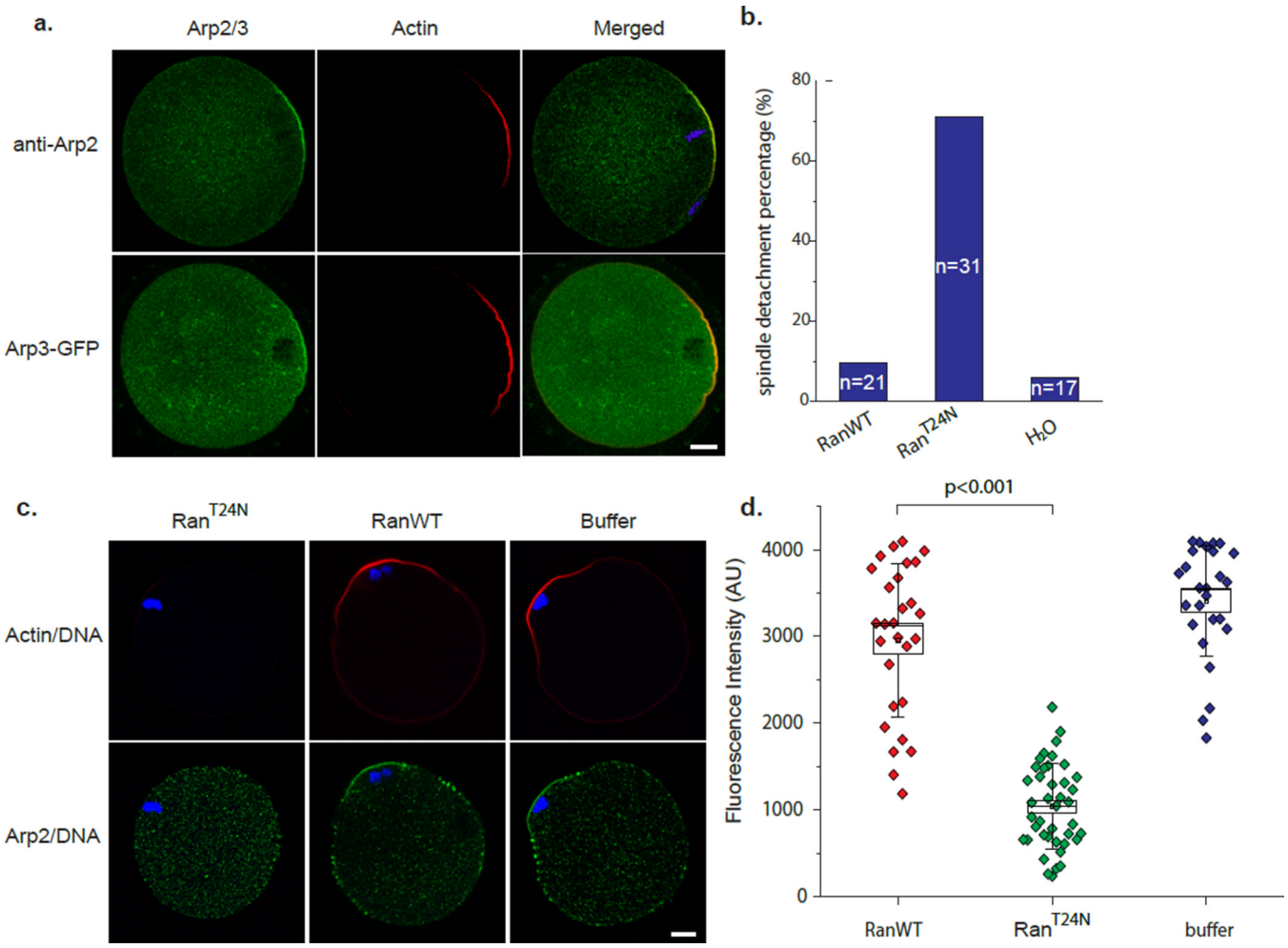

Figure 2. Ran signaling regulates cortical localization of Arp2/3 complex

(a) Cortical cap localization of Arp2/3 complex as determined by anti-Arp2 immuno-staining and Arp3-EGFP expression. In anti-Arp2 panel, blue shows the DAPI staining of chromatin. Scale bar: 10 μm. (b) Quantification of spindle detachment percentage after Ran^{T24N} mutant protein microinjection. (c) Confocal images showing Arp2 dislocalized in Ran^{T24N}-injected oocytes, but not in wild-type Ran (RanWT) or buffer injected oocytes. In this experiment, nocodazole was used to prevent chromosome detachment from the cortex. Scale bar: 10 μm. (d) Quantification of cortical actin cap intensities in Ran-injected oocytes in presence of nocodazole. Box range represents the standard error of the mean; whiskers are the standard deviation; the small square is the mean; and the line inside the box is the median.

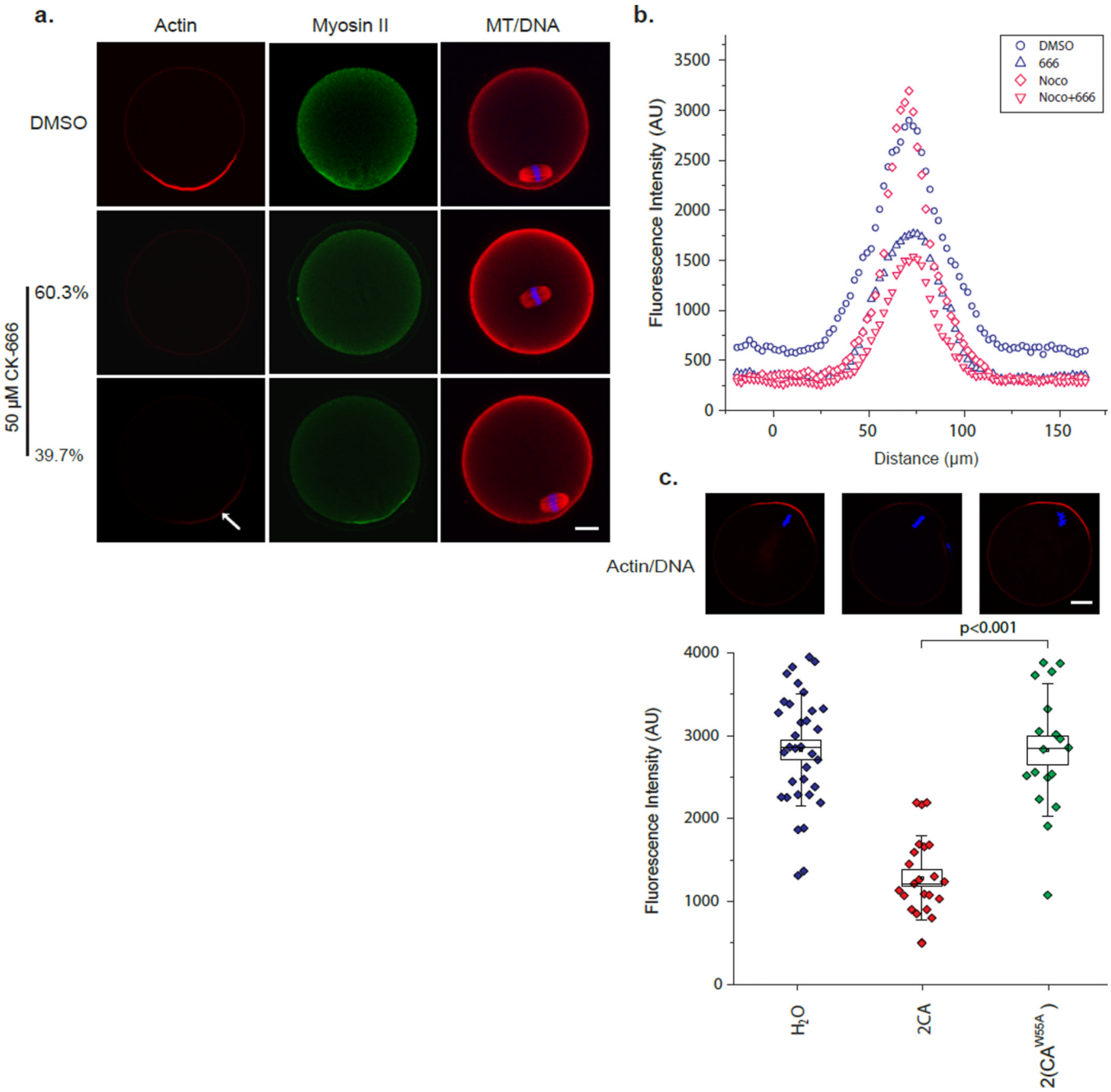

Figure 3. The Arp2/3 complex is required for the majority of F-actin assembly in the cortical cap and for myosin-II ring maintenance

(a) Representative images showing actin and myosin-II localization by phalloidin staining and myosin II immuno-staining, respectively. All actin or myosin-II images were acquired in the same way so that their intensities can be compared. The images were pseudocolored after data acquisition, and the images shown in the same row were from the same oocyte. Note two class of staining patterns, representing 60.3% and 30.7% of total, are shown for CK-666-treated oocytes based on spindle position. (b) Quantification of cortical actin intensities in CK-666 treated and control oocytes (see online Methods). The intensity trace of each group is the mean from 10 oocytes. (c) Representative images and the quantification

of cortical actin cap intensities in 2CA and 2(CA^{W55A})-injected oocytes. Box plots are as described in Fig. 2d legend. Scale bars: 10 μm.

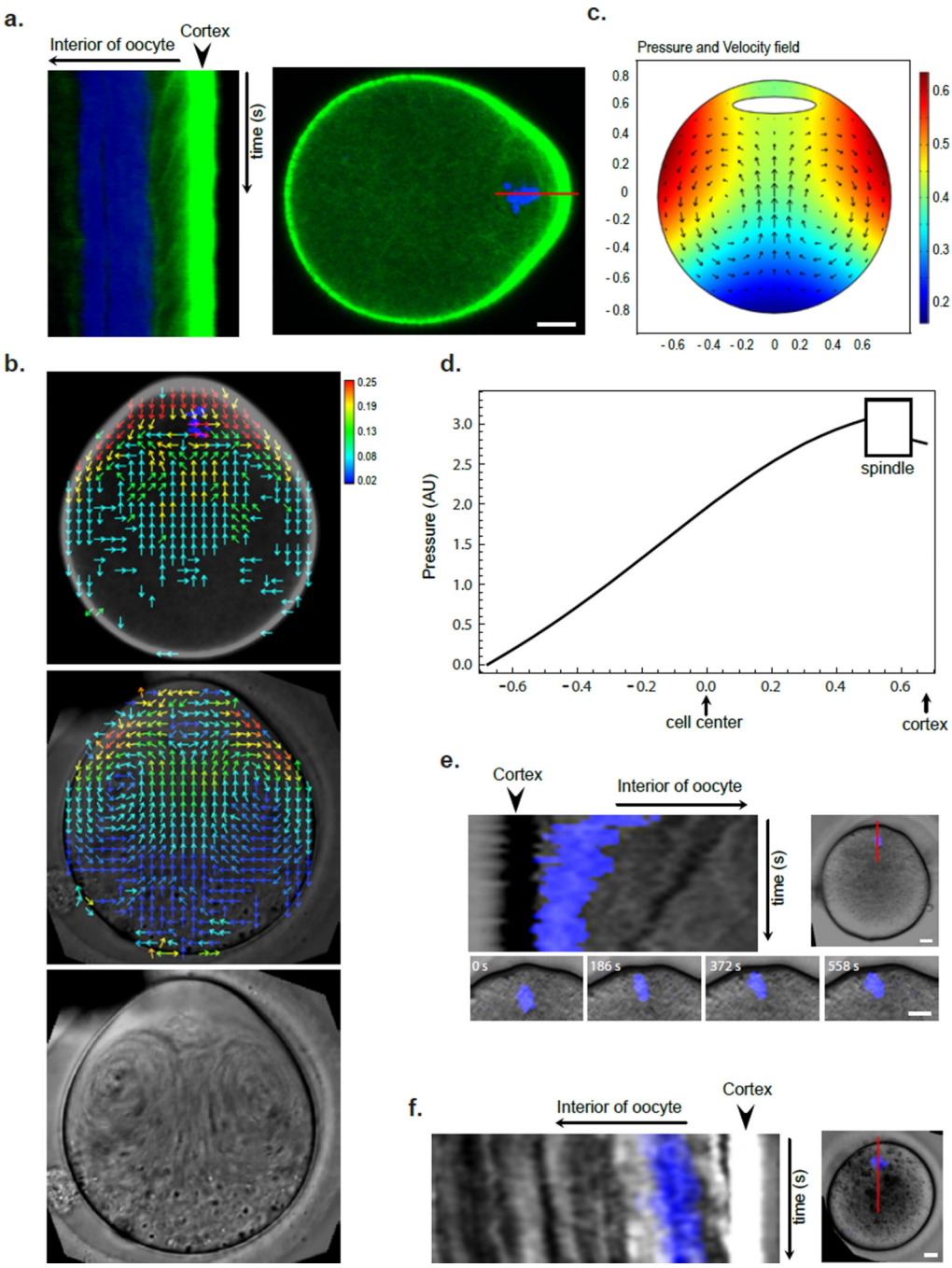

Figure 4. Cytoplasmic streaming powered by Arp2/3 nucleated actin flow generates a net pushing force on spindle

(a) Kymograph showing continuous actin flow away from cortical cap. Movie duration: 1600 s. The right panel shows a still UtCH-GFP image and indicates the line along which the kymograph was generated. Scale bar: 10 μm. (b) Vector maps of actin flow (from a UtCH-GFP movie, top panel) and cytoplasmic streaming (from a DIC movie, middle panel) in MII oocyte obtained using STICS analysis. Heat bar unit: μm/sec. The lower panel is a time projection of the DIC movie showing a swirl pattern of cytoplasmic particles. Scale bar: 10 μm. (c) Pressure and velocity field maps from fluid dynamics simulation of MII oocytes with the source of flow near the cortical cap (see online Methods). (d) A plot of

fluid pressure from the simulation in (c) as a function of the position along the axis through the spindle and cortical cap centers (y axis). Notice the higher pressure at the spindle surface away from the cortical cap than that at the side facing the cortex. (e) Kymograph showing chromatin (blue) movement toward the cortex after spindle disassembly by nocodazole. Movie duration: 2670 s. Notice the similar rate at which a cytolasmic particle moved (dark streak behind the chromatin). Scale bars: 10 μm. (f) Kymograph showing spindle migration back toward the cortex after drug wash-out in a CK-666 treated oocyte. Movie duration: 3450 s. Scale bar: 10 μm.

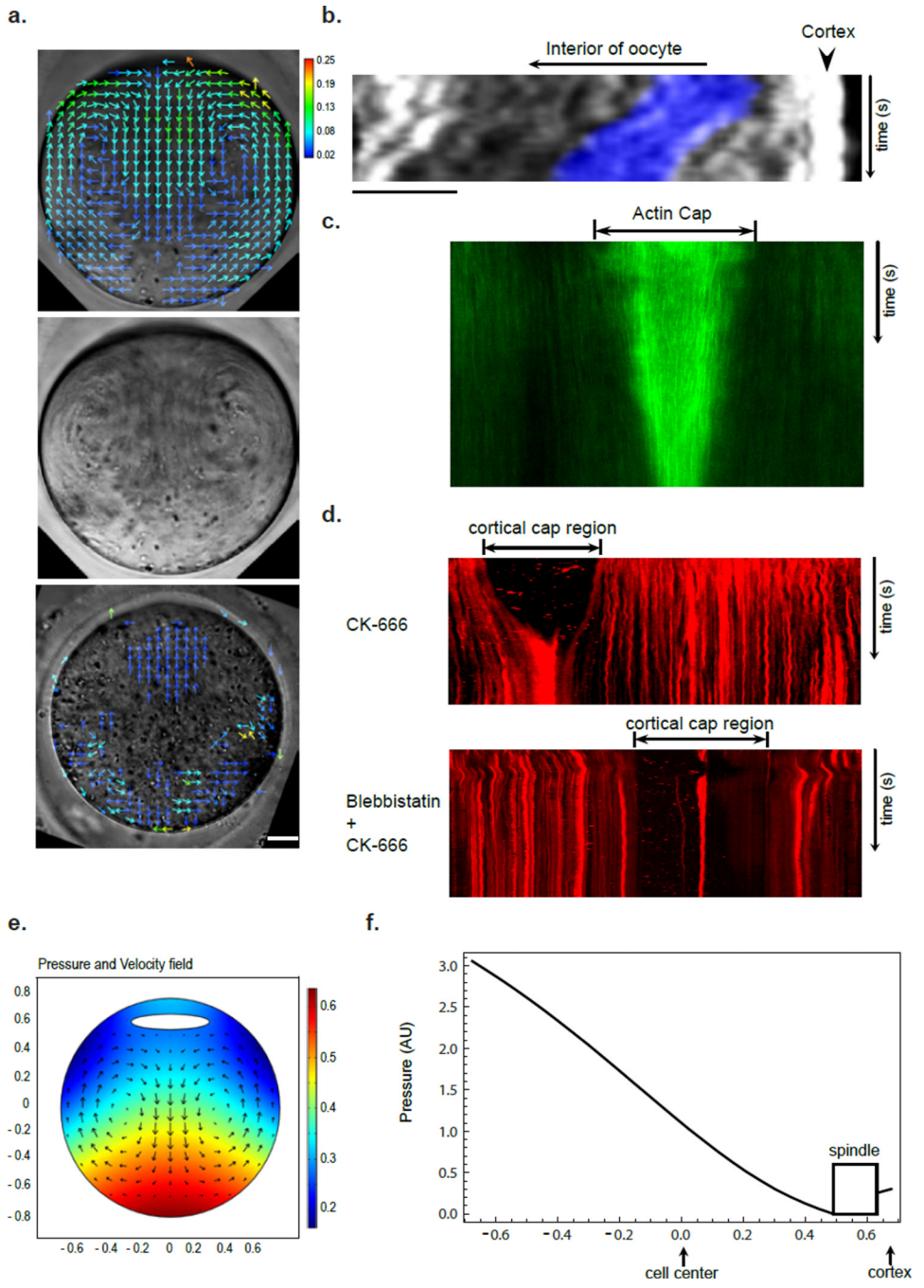

Figure 5. Myosin-II-dependent cortical cap contraction drives MII spindle away from the cortex in the absence of Arp2/3 activity

(a) Vector maps of the reverse cytoplasmic streaming in CK-666-treated oocyte (top panel) and blocking of this reverse streaming by blebbistatin (bottom panel). Heat bar unit: μm/sec. The middle panel is a time projection of the DIC movie showing a swirl pattern of cytoplamic particles in the CK-666-treated oocyte. Scale bar: 10 μm. (b) Kymograph showing the spindle/chromatin (blue) movement away from the cortex at a rate similar to that of cytoplasmic particles after CK-666 addition. Movie duration: 2070 s. Position of the line for kymograph generation is similar to that in Fig. 4e,f. (c) Kymograph generated along a line through the cortex of a UtCH-GFP expressing oocyte showing actin cap contraction

after CK-666 addition. Movie duration: 2245 s. (d) Kymograph generated along a line through the cortex of a Texas red Con-A labeled oocyte showing cortical cap contraction after CK-666 addition along without (top panel) or with blebbistatin (bottom panel). The cap region shows low ConA staining as marked. Movie durations: 4395 s (top) and 4375 s (bottom). (e) Numerical simulation of fluid dynamics showing pressure and velocity fields in oocytes having a reverse cytoplasmic streaming due to cortical cap contraction. (f) A plot of fluid pressure from the simulation in (e) as a function of the position along the axis through spindle and cortical cap centers (y). Notice the higher pressure at the spindle surface facing the cortical cap than that away from the cortex.